

Power Spectrum Estimation from Peculiar Velocity Catalogues

E. Macaulay^{1*}, H. A. Feldman², P. G. Ferreira¹, A. H. Jaffe³,
S. Agarwal², M. J. Hudson^{4,5}, R. Watkins⁶

¹ *Astrophysics, University of Oxford, Denys Wilkinson Building, Keble Road, Oxford OX1 3RH, United Kingdom.*

² *Department of Physics and Astronomy, University of Kansas, Lawrence, KS66045, USA.*

³ *Department of Physics and Astronomy, Imperial College London*

⁴ *Department of Physics and Astronomy, University of Waterloo, Waterloo, ONN2L3G1, Canada.*

⁵ *Perimeter Institute for Theoretical Physics, 31 Caroline St. N., Waterloo, ON, N2L2Y5, Canada.*

⁶ *Department of Physics, Willamette University, Salem, OR97301, USA.*

15 March 2019

ABSTRACT

The peculiar velocities of galaxies are an inherently valuable cosmological probe, providing an unbiased estimate of the distribution of matter on scales much larger than the depth of the survey. Much research interest has been motivated by the high dipole moment of our local peculiar velocity field, which suggests a large scale excess in the matter power spectrum, and can appear to be in some tension with the Λ CDM model. We use a composite catalogue of 4,537 peculiar velocity measurements with a characteristic depth of $33\ h^{-1}\text{Mpc}$ to estimate the matter power spectrum. We compare the constraints with this method, directly studying the full peculiar velocity catalogue, to results from Macaulay et al. (2011), studying minimum variance moments of the velocity field, as calculated by Watkins, Feldman & Hudson (2009) and Feldman, Watkins & Hudson (2010). We find good agreement with the Λ CDM model on scales of $k > 0.01\ h\ \text{Mpc}^{-1}$. We find an excess of power on scales of $k < 0.01\ h\ \text{Mpc}^{-1}$, although with a 1σ uncertainty which includes the Λ CDM model. We find that the uncertainty in the excess at these scales is larger than an alternative result studying only moments of the velocity field, which is due to the minimum variance weights used to calculate the moments. At small scales, we are able to clearly discriminate between linear and nonlinear clustering in simulated peculiar velocity catalogues, and find some evidence (although less clear) for linear clustering in the real peculiar velocity data.

Key words: cosmology: large scale structure of the universe – cosmology: observation – cosmology: theory – galaxies: kinematics and dynamics – galaxies: statistics

1 INTRODUCTION & BACKGROUND

The peculiar velocities of galaxies are a powerful cosmological probe, which directly traces the underlying dark matter distribution (independent of galaxy bias) and is also sensitive to scales much larger than the size of the survey. Recent interest in peculiar velocities has been driven by the high dipole moment of our local velocity field, which can appear to be in some tension with the Λ CDM model. The Λ CDM model indicates that we should expect a peculiar velocity dipole of magnitude around $100\ \text{km s}^{-1}$, although many independent peculiar velocity surveys

show evidence for a bulk flow at low redshift of around $400\ \text{km s}^{-1}$ in the direction $l = 280\ b = 10$ degrees (Hudson et al. 2004; Watkins, Feldman & Hudson 2009; Feldman, Watkins & Hudson 2010; Ma, Gordon & Feldman 2010). However, Nusser & Davis (2011) find evidence for a flow more commensurate with Λ CDM of around $260\ \text{km s}^{-1}$ (in a similar direction as the other bulk flow results). Recently, Abate & Feldman (2011) found evidence for an extremely high bulk flow of around $4000\ \text{km s}^{-1}$ at redshift ~ 0.3 , in a similar direction to other low redshift bulk flows. Kashlinsky et al. (2010) find a bulk flow of around $1000\ \text{km s}^{-1}$ extending to $z \simeq 0.2$ from kinematic Sunyaev-Zel’dovich measurements.

* email: edward.macaulay@astro.ox.ac.uk

In addition to the high dipole moment, there also ap-

pears to be a low shear of the velocity field (Jaffe & Kaiser 1995; Feldman, Watkins & Hudson 2010), which indicates that the density contrast responsible for the velocity dipole is on extremely large scales. At the depths of the peculiar velocity surveys (up to $100 h^{-1}\text{Mpc}$), this suggests an excess density contrast on scales $\sim 1 h^{-1}\text{Gpc}$. The volume of space probed by galaxy redshift surveys (e.g. Cole et al. 2005; Reid et al. 2010 and Blake et al. 2010) is currently too small to robustly constrain clustering on these scales, although Thomas, Abdalla & Lahav (2010) found evidence for excess large scale power in the MegaZ photometric redshift survey. Measurements of the CMB can probe anisotropies on these large scales (Hlozek et al. 2011), although to compare to results at low redshift, the growth of these anisotropies must be assumed, which depends on the cosmological model.

There are many possible explanations for the high dipole moment, ranging from systematic effects to more exotic explanations invoking extended cosmology or modified gravity. Hudson et al. (2004) considered systematic effects in the SMAC peculiar velocity survey, such as a dipole variation in the velocity dispersion, galactic extinction, and calibration across different observations. They found that systematic effects could account for at most half of the high dipole moment of the SMAC survey, leaving a dipole moment which is still at least three times higher than the ΛCDM expectation. There are many theoretical possibilities to extend the ΛCDM model to produce a large scale excess of power and a peculiar velocity dipole, such as modifications to gravity, (Ayaita, Weber & Wetterich 2009; Khoury & Wyman 2009), dark energy clustering (Potter & Chongchitnan 2011), vorticity, (Palle 2010) or ‘tilted’ universes (Mersini-Houghton & Holman 2009; Kashlinsky et al. 2010; Ma, Gordon & Feldman 2010). In this work we do not address any theoretical explanation in particular, but by using the peculiar velocity data to constrain the power spectrum in model independent band-powers we aim to provide results which will be useful to constrain a range of explanations for the high dipole.

Jaffe & Kaiser (1995), Kolatt et al. (1996), Zaroubi et al. (1997), Kolatt & Dekel (1997), Zaroubi et al. (2001) and Silberman et al. (2001) have used peculiar velocity surveys to infer the matter power spectrum directly at $z = 0$. More recently in Macaulay et al. (2011), we inferred the underlying power spectrum from moments of the peculiar velocity field from Watkins, Feldman & Hudson (2009) and Feldman, Watkins & Hudson (2010), specifically in the context of understanding the high bulk flow. One of our main findings was that the excess of power indicated by the anomalously high dipole moment was dramatically reduced when the shear and octupole moments were also included. This leads us to ask if the correspondence with the ΛCDM model would be improved if we were to hypothetically include higher still moments of the velocity field. That is the motivation for this work, although we take the approach used by Jaffe & Kaiser (1995) to analyse peculiar velocity catalogues directly, without compressing the data into moments.

Recently, Abate & Erdoğdu (2009) applied a similar formalism to constrain the modified gravity parameter γ . Similarly Ma, Gordon & Feldman (2010) used a similar formalism to fit for parameters of the dipole moment and velocity dispersion parameter. In both cases, a fiducial ΛCDM

power spectrum was assumed, and additional parameters of interest were allowed to vary. The key difference between those papers and this work is that here we treat the underlying power spectrum as a set of free parameters, as opposed to fitting extra parameters for additional effects beyond a fixed power spectrum. In this way, we obtain new constraints on the power spectrum which are independent of the fiducial cosmology.

2 METHOD

In this paper we consider two distinct methods to relate peculiar velocity measurements to large scale structure: A maximum likelihood based approach to analyse a full peculiar velocity catalogue (the ‘catalogue’ method), and an alternative approach studying minimum-variance moments of the velocity field (the ‘moments’ method).

As well as an apparent radial velocity due to the Hubble flow, galaxies also have a peculiar velocity towards local over-densities of matter. This peculiar velocity field $\mathbf{v}(\mathbf{r})$ can be related to the matter density contrast δ by

$$\mathbf{v}(\mathbf{r}) = \frac{f_g H_0}{4\pi} \int d^3\mathbf{r}' \delta(\mathbf{r}') \frac{(\mathbf{r}' - \mathbf{r})}{|\mathbf{r}' - \mathbf{r}|^3} \quad (1)$$

where f_g is the growth rate of the density contrast, $\partial \ln \delta / \partial \ln a$, and a is the scale factor (Peebles 1993). The density contrast is defined in terms of the ratio of the density at \mathbf{r} , ρ , to the average density $\bar{\rho}$, so that $\delta = \rho / \bar{\rho}$.

We can measure the peculiar velocity via the effect it has on the redshift of the galaxy. The redshift z of a galaxy is given by a contribution from the Hubble flow, $H_0 r$, and the line of sight component of the peculiar velocity S :

$$cz = H_0 r + S \quad (2)$$

where, for a galaxy labelled m , at position \mathbf{r}_m , we have the line of sight peculiar velocity, S_m given by

$$S_m = \hat{\mathbf{r}}_m \cdot \mathbf{v}(\mathbf{r}_m) \quad (3)$$

where $\hat{\mathbf{r}}_m$ is a unit vector in the direction of galaxy m . To measure S we thus need to combine the redshift of the galaxy with an *independent* measure of the distance r . In principle, we can calculate the peculiar velocity of any galaxy for which we have the luminosity distance, measured using distance indicators such as supernovae (SN), Tully-Fisher (TF) (Tully & Fisher 1977) or Fundamental-Plane (FP) (Dressler et al. 1987) measurements. Individual uncertainties on luminosity distances are typically rather large (5% for SN, and around 10 to 20% for TF and FP), which propagates to a very large uncertainty in the peculiar velocity.

2.1 Maximum Likelihood Catalogue Method

We now consider how to relate a catalogue of peculiar velocity measurements S_m to large scale structure, following the method as presented in Jaffe & Kaiser (1995). The method is based on a likelihood framework, where the likelihood \mathcal{L} is given by

$$\mathcal{L} = \frac{1}{2\pi^{N/2} |R_{mn}|^{1/2}} \exp \left(-\frac{1}{2} S_m R_{mn}^{-1} S_n \right) \quad (4)$$

where R_{mn} is the covariance matrix for the peculiar velocity measurements, for a catalogue of N galaxies. The covariance matrix is split into two components, a ‘velocity’ and an ‘error’ term:

$$R_{mn} = R_{mn}^{(v)} + R_{mn}^{(e)}. \quad (5)$$

$R_{mn}^{(v)}$ models the coherent large scale structure, and $R_{mn}^{(e)}$ is a noise component to account for nonlinear velocity dispersion σ_* , and uncertainty in each peculiar velocity measurement σ_m . If we assume that the measurement errors are uncorrelated, $R_{mn}^{(e)}$ simply contributes these uncertainties to the diagonal of the covariance matrix, and is given by

$$R_{mn}^{(e)} = (\sigma_m^2 + \sigma_*^2) \delta_{mn} \quad (6)$$

where δ_{mn} is a Kronecker delta. The large scale structure of interest enters via the ‘velocity’ component of the covariance matrix, and is given by

$$R_{mn}^{(v)}(k) = \int \frac{4\pi k^2 dk}{(2\pi)^3} P_v(k) f_{mn}(k) \quad (7)$$

where $P_v(k)$ is the velocity power spectrum, which is related to the matter power spectrum by

$$P_v(k) = \left(\frac{H_0 a}{k}\right)^2 f_g^2 P(k). \quad (8)$$

Here a is the scale factor. The window function $f_{mn}(k)$ is given by

$$f_{mn}(k) = \hat{r}_{m,i} \hat{r}_{n,j} \int \frac{d^2 \hat{k}}{4\pi} \hat{k}_i \hat{k}_j e^{ik\hat{k} \cdot (\mathbf{r}_m - \mathbf{r}_n)} \quad (9)$$

and can be calculated analytically in terms of trigonometric functions. A derivation of f_{mn} is presented in Ma, Gordon & Feldman (2010). The general approach we take is to map out the likelihood in terms of parameters of the power spectrum. We next consider an analogous method to analyse moments of the velocity field, before considering parametrisation of the power spectrum any further, since the parametrisation is common to both methods.

2.2 Minimum Variance Moments Method

In this paper we directly compare results between the maximum likelihood catalogue method to an alternative method studying moments of the velocity field, from Macaulay et al. (2011). We can consider the velocity field as a Taylor expansion, given by:

$$v_i(\mathbf{r}) = U_i + U_{ij} r_j + U_{ijk} r_j r_k + \dots \quad (10)$$

where U_i is the dipole moment of the velocity field (often called the ‘bulk flow’), and provides most information about the largest scale fluctuations. U_{ij} is the shear of the velocity field, sensitive to intermediate scales. U_{ijk} is the octupole moment, and is sensitive to scales less than the size of the survey. The relative sensitivity of each moment is shown in Figure 1. Since we can only measure the line of sight component of each peculiar velocity, each individual measurement must be weighted according to the component of the moment it is sensitive to. Watkins, Feldman & Hudson (2009) and Feldman, Watkins & Hudson (2010) developed new ‘minimum variance’ weights to estimate the velocity of the volume traced by the galaxies in the survey. These weights

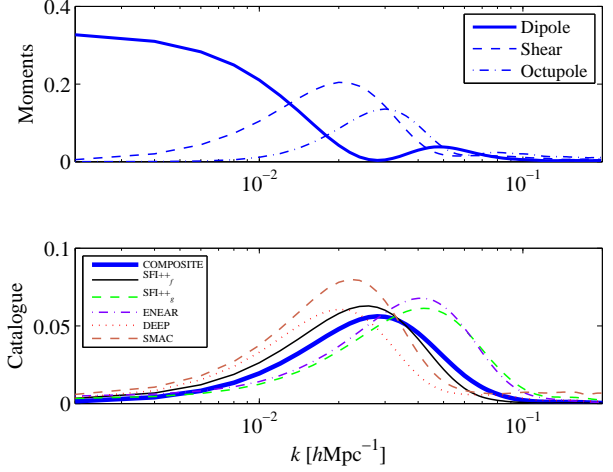


Figure 1. Comparing sensitivity to different scales for the moments and catalogue methods. For the moments panel, we plot the average of the diagonal of the covariance matrix for the dipole, shear and octupole terms, for COMPOSITE. Since the moments are designed to be orthogonal, the diagonal of the covariance matrix gives an indication of the scales at which the moments are most sensitive. For the catalogue panel, the diagonal of the covariance matrix is $1/3$, so we plot the sum of the entire covariance matrix, normalised by the square of the number of galaxies in each catalogue, which illustrates the scales at which the window function is sensitive. The sub-catalogues which span the greatest distance, DEEP and SMAC, are most sensitive to largest scales, while the shallowest catalogues, SFI++_g and ENEAR, are most sensitive to smaller scales.

are designed to minimise the effects of small scale motions, to provide a better estimate of the large scale velocities. We do not reproduce the derivations of the weights here; the method is presented in Watkins, Feldman & Hudson (2009) for the dipole and extended in Feldman, Watkins & Hudson (2010) for the shear and octupole.

With this method, the data consists of the three components of the dipole vector, six independent components of the shear, and ten independent components of the octupole. We take a similar approach as with the catalogue method, splitting the covariance matrix into ‘velocity’ and ‘error’ terms. The ‘velocity’ term is now given by

$$R_{pq}^{(v)} = \frac{f_g^2}{2\pi^2} \int dk P(k) \mathcal{W}_{pq}^2(k) \quad (11)$$

where p and q index the 19 independent moments. The window function $\mathcal{W}_{pq}^2(k)$ is sensitive to different scales for the dipole, shear and octupole, as plotted in Figure 1. We construct a likelihood in exactly the same manner as the catalogue method, in terms of parameters of a power spectrum, which we now consider.

2.3 Power Spectrum Parametrisation

Ultimately, we wish to constrain parameters of the underlying matter power spectrum. There are many choices for ways to parametrise the power spectrum. A popular choice in many earlier works was the power spectrum shape parameter Γ , the matter density Ω_m and the power spec-

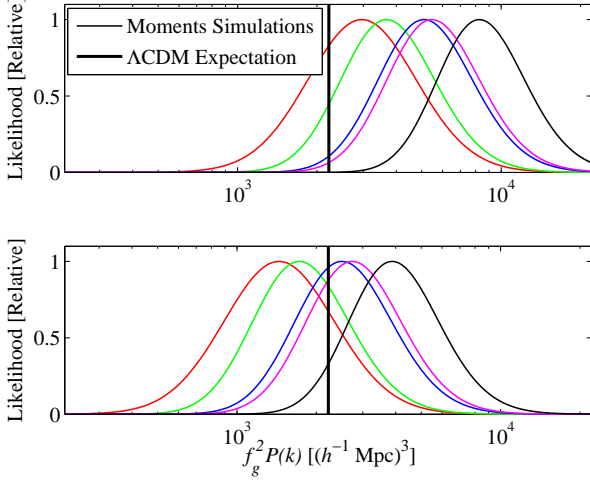


Figure 2. The effect of band shape. In the upper Figure, when using the constant amplitude of a single flat band-power to parametrise the power spectrum, we find a systematic excess compared to the average Λ CDM power spectrum in the same k range. However, when we use the amplitude of the Λ CDM power spectrum, A_α as a parameter, we find no systematic deviation from the $A_\alpha = 1$ expectation.

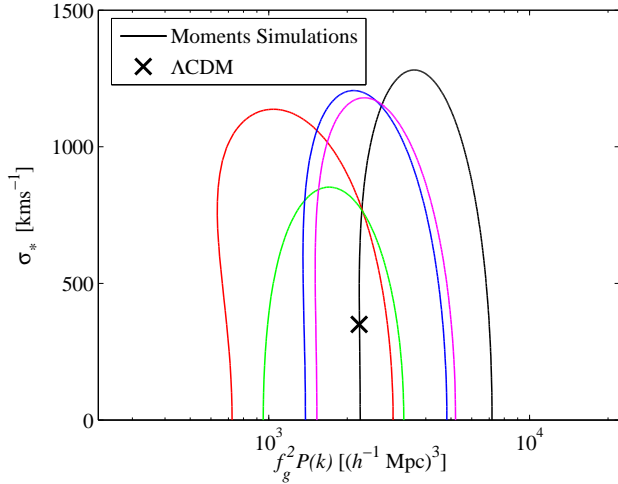


Figure 3. One standard deviation contours for one power spectrum band and the velocity dispersion σ_* , for moments generated from a simulated velocity field. The contours are fairly insensitive to the choice of σ_* . Since compressing the velocity field into moments is insensitive to small scale effects, these contours are consistent with $\sigma_* = 0$. The 1d likelihood distributions are for a fixed σ_* of 200 km s^{-1} .

trum normalization at $8 h^{-1} \text{Mpc}$, σ_8 (Jaffe & Kaiser 1995; Kolatt & Dekel 1995). Silberman et al. (2001) opted for a band-power parametrisation, which is the approach we take here, in terms of band-powers, P_α , so the power spectrum is given by

$$P(k) = \begin{cases} P_\alpha & k_\alpha < k < k_{\alpha+1} \\ 0 & \text{otherwise.} \end{cases} \quad (12)$$

The velocity covariance matrix is then

$$R_{mn}^{(v)}(k) \approx \frac{(H)^2}{2\pi^2} f_g^2 \sum_\alpha P_\alpha \mathcal{K}_\alpha \quad (13)$$

where \mathcal{K} is given by

$$\mathcal{K}_\alpha = \int_{k_\alpha}^{k_{\alpha+1}} dk f_{mn}(k) \quad (14)$$

This parametrisation is directly sensitive to the combination of $f_g^2 P_\alpha$. To directly constrain $P(k)$, we must either assume a fiducial growth rate, or marginalise over other measurements of the growth rate. For generality, we choose to treat the combination of $f_g^2 P_\alpha$ as a parameter.

In Macaulay et al. (2011), we used flat band-powers. This parametrisation was sufficient to demonstrate the large effect of including just the dipole, or higher moments of the velocity field. However, in the widest, single band parametrisation, the flat bands can introduce an apparent artificial shift towards an excess of power, shown in the upper panel of Figure 2. We find that when we factor in a fiducial Λ CDM power spectrum into the window function, $P_{\text{fid}}(k)$, and allow a constant amplitude of this power spectrum, A_α , to vary, we obtain an amplitude which is consistent with Λ CDM. The kernel in this case is

$$\mathcal{K}_\alpha = \int_{k_\alpha}^{k_{\alpha+1}} dk f_{mn}(k) P_{\text{fid}}(k) \quad (15)$$

so our velocity covariance matrix is now

$$R_{mn}^{(v)} \approx \frac{(H)^2}{2\pi^2} f_g^2 \sum_\alpha A_\alpha \mathcal{K}_\alpha \quad (16)$$

where our parameter is now A_α , the amplitude of the fiducial power spectrum in each band. We thus expect $A_\alpha = 1$ in all bands for a Λ CDM velocity field. To more easily compare A_α to expectations, we multiply the results by the mean of the power spectrum in each band, $\langle P_\alpha \rangle$, given by

$$\langle P_\alpha \rangle = \frac{\int_{k_\alpha}^{k_{\alpha+1}} dk P_{\text{fid}}(k)}{k_{\alpha+1} - k_\alpha}. \quad (17)$$

Although this parametrisation specifies the shape of the power spectrum within each band, we see in Section 4 in simulated catalogues that the method is fairly robust to the choice of fiducial power spectrum. We find that the catalogue method is sensitive to the velocity dispersion parameter, and thus treat it as a free parameter in the manner of Ma, Gordon & Feldman (2010). To directly compare between the catalogue and moments method, we repeat much of the analysis of Macaulay et al. (2011) with σ_* as a free parameter, although we find with results from velocity moments that marginalising over the velocity dispersion parameter has only a very small effect. Similarly, in this paper we now consider the combination of $f_g^2 P_\alpha$ as a parameter for both methods, as opposed to marginalising over the growth rate as in Macaulay et al. (2011). We assume a fiducial value for the velocity dispersion of 350 km s^{-1} .

3 PECULIAR VELOCITY DATA

We primarily study the COMPOSITE peculiar velocity catalogue, which consists of 4537 individual peculiar velocity measurements, and a characteristic depth of 33

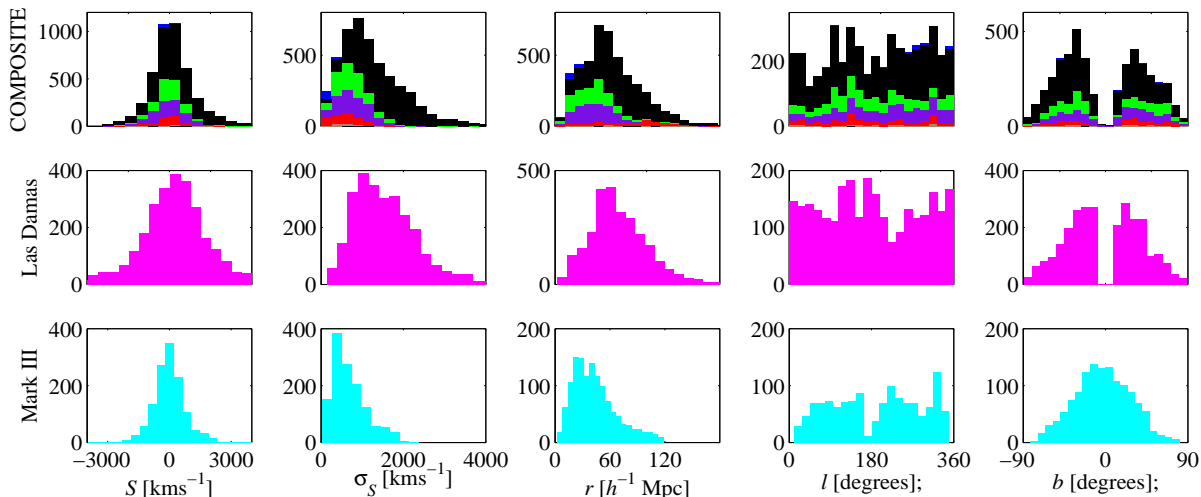


Figure 4. Histograms of the real surveys, and the Las Damas and Mark III simulated surveys, illustrating the distribution of line of sight peculiar velocities, S , uncertainty in S , σ_S , distance r , and coordinates l and b . The COMPOSITE survey is plotted as a stacked histogram and is comprised of the SFI++_f (black), SFI++_g (green), ENEAR (purple), DEEP (red), and SMAC (brown) surveys.

h^{-1} Mpc, compiled by Feldman, Watkins & Hudson (2010). The COMPOSITE catalogue is composed of several sub-catalogues, which we also consider individually. The largest sub-catalogue is the SFI++ sample, which consists of 3456 TF measurements. We analyse the field galaxies and groups in the SFI++ sample separately, as SFI++_f (2720 galaxies) and SFI++_g (736 measurements) (Masters et al. 2006; Springob et al. 2009a,b). We also study the combined DEEP catalogue, compiled by Watkins, Feldman & Hudson (2009), which consists of 294 of the deepest peculiar velocity measurements and the ENEAR catalogue (da Costa et al. 2000). The smallest catalogue we consider individually is the SMAC catalogue (Hudson et al. 2004), which is a sub-set of the DEEP catalogue.

We test our procedures on peculiar velocity catalogues generated from Λ CDM simulations. We analyse the set of 20 simulated Mark III catalogues¹ drawn from realisations of the Virgo simulation (Kolatt et al. 1996), consisting of 1300 entries each (some of the catalogues consisted of slightly more than 1300 entries - these were trimmed to 1300 for consistency). We also study six simulated catalogues from the Las Damas simulation (McBride et al. 2011, in prep.), designed to resemble the SFI++_f catalogue with 2720 entries. Histograms of the real and simulated surveys are shown in Figure 4.

We study the simulated data sets with both the catalogue and moments method. We analyse the real data with the catalogue method for the combined COMPOSITE set, and the five sub-catalogues. We find that the sub-catalogues are too small to reliably study the moments alone, so we present results here with the moments method only for the COMPOSITE catalogue.

4 RESULTS

4.1 Simulated Data

We begin by testing our method on peculiar velocity catalogues generated from Λ CDM simulations. We start the analysis with the simplest parametrisation: one band-power. We choose a window function range of $k = 0.002$ to $0.196 h^{-1}$ Mpc, to match the k range used in Macaulay et al. (2011). We also include the velocity dispersion as a free parameter. Results are shown in Figure 5.

We find that for this band-power parametrisation, the velocity dispersion is uncorrelated with the power spectrum amplitude. The velocity dispersion is slightly higher than the Λ CDM expectation for the Las Damas mocks, although it is lower in the Mark III mocks. In both sets of mocks, we note a small systematic shift from the Λ CDM expectation. As this shift is in opposite directions for the Mark III and Las Damas mocks, it seems reasonable to conclude that this may be due to the many particularities of generating a mock catalogue from an underlying power spectrum, as opposed to a systematic shift introduced by our method. In other words, the Mark III and Las Damas mocks taken together surround the Λ CDM expectation well. Following Macaulay et al. (2011), we next consider a parametrisation with three band-powers, spanning the same k range with bands evenly spaced in $\log k$. The results are shown in Figure 6.

We will refer to the bands from the largest scales to the smallest scales as bands 1 to 3. We find that the uncertainty in band 1 is larger in the simulated data with the catalogue method than the moments method (not plotted). The uncertainty in band 1 is particularly important for understanding the high dipole moment, and will be discussed further in Section 5. Both sets of catalogues are much more sensitive in band 3 than with the moments method; we thus decide to extend that band-power parametrisation by adding two

¹ downloaded from <http://www.mpa-garching.mpg.de/NumCos/CR/Download/index.html>

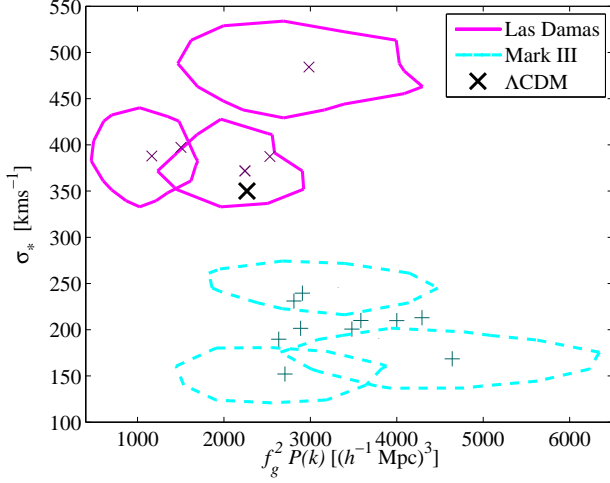


Figure 5. Constraints on the velocity dispersion parameter σ_* and one band-power, in the range $k = 0.002$ to $0.196 \ h^{-1}\text{Mpc}$, for *simulated* peculiar velocity surveys from the Las Damas and Mark III simulations. The markers represent the peak of the likelihood for each catalogue. The contours are 1 standard deviation uncertainty about the peak likelihood, which we have only plotted for three catalogues for each simulation set, to prevent the plot from becoming overcrowded. Similarly, we only plot results for 10 of the Mark III catalogues. These uncertainty ranges are typical for the points plotted here.

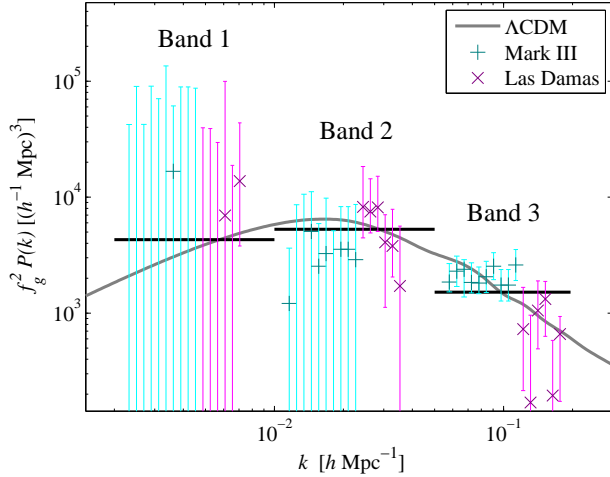


Figure 6. Results from the Mark III and Las Damas mocks in three band-powers. The velocity dispersion was varied as a free parameter, and marginalized over in these results. The grey curve is the ΛCDM power spectrum. The horizontal black lines span the k ranges of the band-powers, and indicate the average value of the power spectrum across this range. The results should be compared directly to these. The markers are the marginalized results for each band-power, for each of the Mark III and Las Damas surveys. The k location within each band is arbitrary; each point should be fully considered equally at the centre of the band, spanning the full width.

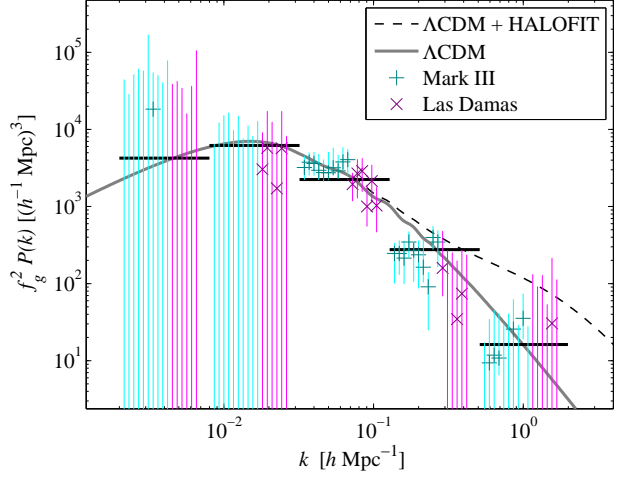


Figure 7. As Figure 6, but with two additional bands added at smaller scales. The smallest scale band is at scales for which galaxy power spectra must be corrected for (e.g., with Halofit). With the peculiar velocity method, we are sensitive to the total matter distribution, and can thus directly probe the *linear* power spectrum, without accounting for halo corrections.

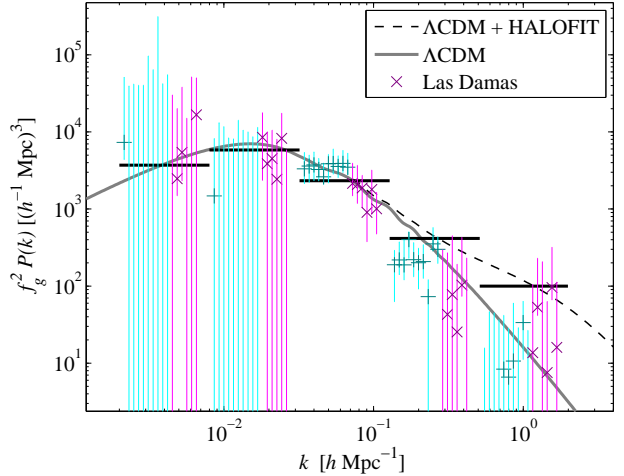


Figure 8. As Figure 7, but with a fiducial power spectrum corrected with Halofit. The black bars now represent the mean value of the Halofit fiducial power spectrum which was factored into the window function. The data still favor the linear power spectrum, indicating that the method is robust to the choice of fiducial power spectrum.

more bands (4 and 5) at smaller scales. Results are shown in Figure 7.

We find that band 5 is anti-correlated with the velocity dispersion parameter. This is not surprising, given the $\sim 5 \ h^{-1}\text{Mpc}$ scales spanned by this band. We are encouraged to see a difference at over 1σ from the nonlinear Halofit (Smith et al. 2003) corrections to the galaxy power spectra, illustrating the ability of peculiar velocity measurements to directly probe the underlying *linear* matter distribution. As a test, we repeat the results in Figure 7 assuming a fiducial Halofit corrected power spectrum to factor into the window function. The results are shown in Figure 8. Encouragingly,

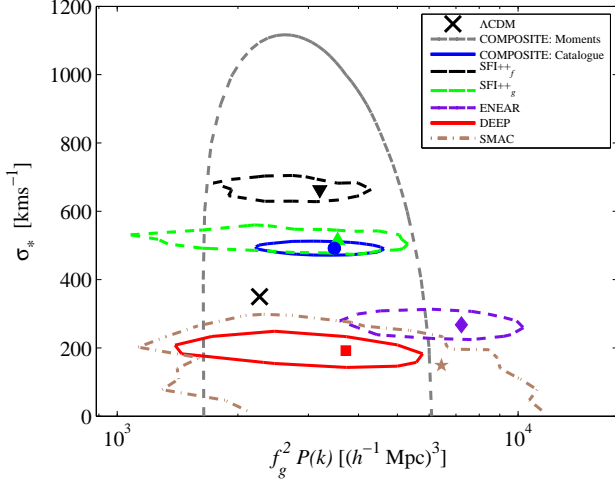


Figure 9. 1 standard deviation contours from the real data, parametrised in terms of the velocity dispersion σ_* and one band-power, in the range $k = 0.002$ to $0.196 \, h^{-1}\text{Mpc}$. There is a slight excess of power in all the catalogues, although within the 1σ level for most.

we see in the smallest two bands that the data still favour the linear power spectrum.

4.2 Real Data

We now consider results from real peculiar velocity surveys. We start with the one band-power and velocity dispersion parametrisation, shown in Figure 9.

Using the ΛCDM shape band, we find a slightly lower average amplitude than the flat band result from Macaulay et al. (2011). Although we note a small excess, the ΛCDM value is now well within the 1σ uncertainty range of the moments result. We find that the results for the velocity dispersion agree well with similar results from Ma, Gordon & Feldman (2010). We find a smaller uncertainty in the band-power with the catalogue method than the moments method, and a much improved constraint on the velocity dispersion parameter. We next consider a three band parametrisation, shown in Figure 10.

With the moments method, band 3 was merely an upper limit - it is well constrained by the catalogue method. The low shear of the velocity field caused band 2 to be lower than the ΛCDM expectation. When we now analyse the full catalogue, the band agrees extremely well with the ΛCDM expectation. We still observe an excess of power in band 1, although the lower bound is not constrained here. These results are discussed further in Section 5. We next extend the parametrisation with two smaller bands, as before with the simulated catalogues. The results are plotted in Figure 11, and presented for COMPOSITE in Table 1. We find good agreement with ΛCDM in bands 3 and 4. We find that bands 1 and 2 are anti-correlated.

4.2.1 Comparison to Silberman et al. (2001)

We also test our methodology by reproducing the results of Silberman et al. (2001), to which our method is similar. We

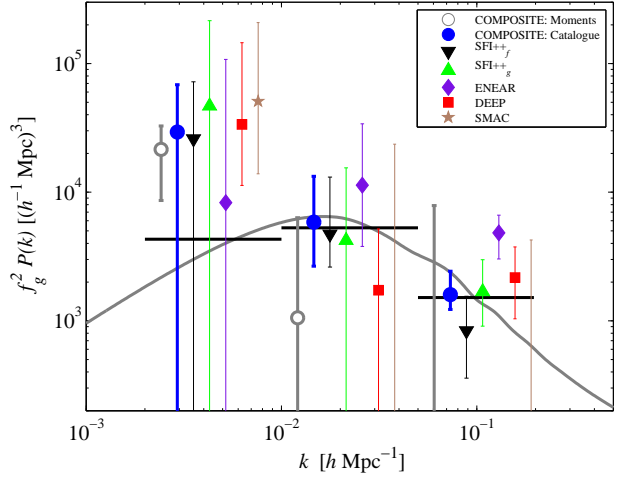


Figure 10. As Figure 6, for the real peculiar velocity catalogues. As before, the k position of each point within the bin is arbitrary, and each point should be fully considered at the centre of each band. The points have been ordered in each band from left to right by the number of galaxies in each catalogue. We also plot results from the moments analysis of the COMPOSITE catalogue.

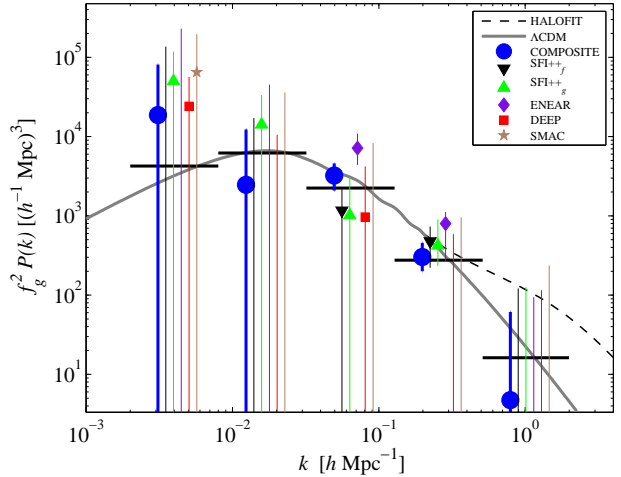


Figure 11. As Figure 7, now for real data. In band 1 we see a slight excess of power, although the uncertainty includes the ΛCDM model at the 1σ level. Band 5 favours the linear clustering power spectrum over the nonlinear model.

change our bands as follows, to match the bands used in their work: For $k \leq 0.02 \, h\text{Mpc}^{-1}$ we use a ΛCDM band, which we do not vary. In the range $0.02 < k \leq 0.07$ and $0.07 < k \leq 0.2 \, h\text{Mpc}^{-1}$ we use two independent flat bands of constant amplitude. For $k > 0.2 \, h\text{Mpc}^{-1}$ we use a power law band, $A_\alpha k^n$. The spectral slope n is set to -0.95 for the simulated Mark III catalogues, and to -1.4 for the real SFI++_f catalogue, and the free parameter A_α is varied. The results are shown in Figure 12. We reproduce the slight decrement at $k \sim 0.1 \, h\text{Mpc}^{-1}$ as noted by Silberman et al. (2001), which we also observe in the SFI++_f catalogue in band 3 of our 5 band parametrisation in Figure 11.

Band	$f_g^2 P(k) [(h^{-1}\text{Mpc})^3]$	
	ΛCDM	COMPOSITE
1	4.2×10^3	$1.9^{+6.2}_{-1.9} \times 10^4$
2	6.2×10^3	$2.5^{+9.9}_{-2.5} \times 10^3$
3	2.2×10^3	$3.2^{+1.4}_{-1.1} \times 10^3$
4	2.8×10^2	$3.0^{+1.5}_{-1.0} \times 10^2$
5	1.6×10^1	$0.5^{+5.7}_{-0.5} \times 10^1$

Table 1. Results for the COMPOSITE catalogue five-band parametrisation, as plotted in Figure 11. Although the high dipole velocity leads to an excess of power by over a factor of 4 in band 1, the uncertainty includes the ΛCDM model within the 1σ uncertainty level.

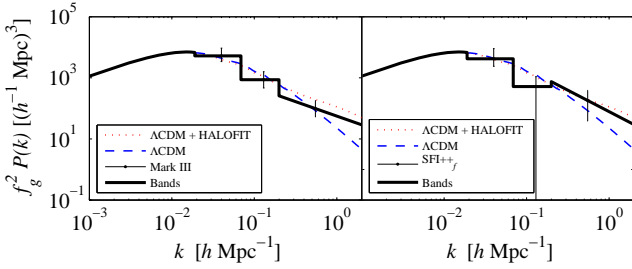


Figure 12. Analyzing a simulated Mark III catalogues with the parametrisation of Silberman et al. (2001). The results we find here agree well with the results in Figure 7 of Silberman et al. (2001).

4.3 Fitting a Velocity Dipole

In the three band model, we find that the uncertainty in band 1 is larger with the catalogue method than with the moments method. We see these results in the simulated catalogues, but it is particularly important to understand the result in the COMPOSITE catalogue since it is closely related to the high velocity dipole. As can be seen in Figure 1, the catalogue method window function is most similar to the window function of the shear moment, and (relatively) not as sensitive to the scales probed by band 1. To try and understand these results, we use our maximum likelihood method to estimate the dipole, to compare to the minimum variance dipole of Feldman, Watkins & Hudson (2010). Instead of varying the power spectrum, we fix the power spectrum at the fiducial ΛCDM value and minimise parameters of the dipole, as analysed by Ma, Gordon & Feldman (2010). We find that it is not possible to simultaneously constrain the three band-power spectrum and a velocity dipole. Following Ma, Gordon & Feldman (2010), we model the dipole \mathbf{U} by subtracting the line of sight component of the dipole to each galaxy in the catalogue from its line of sight peculiar velocity, S_n , to obtain a ‘tilted’ velocity, p_n

$$p_n = S_n - \hat{r}_n \cdot \mathbf{U} . \quad (18)$$

We parametrise the dipole bulk flow as $\mathbf{U} = \{U_r, U_l, U_b\}$, where U_r is the magnitude of the bulk flow (in km s^{-1}), and U_l and U_b are the direction of the flow in degrees (galactic coordinates). We also include the velocity dispersion σ_* as a

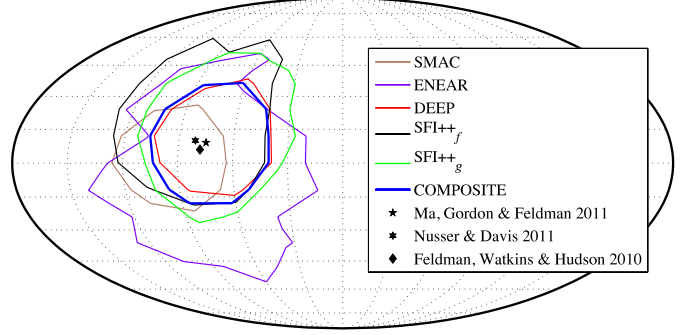


Figure 13. The direction of the best-fitting velocity dipole in the catalogues, (in a Mollweide projection of the sky in galactic coordinates). The contours represent 1 standard deviation levels on the dipole direction angles U_l and U_b found in the peculiar velocity catalogues. The direction agrees with other results from Feldman, Watkins & Hudson (2010), Ma, Gordon & Feldman (2010) and Nusser & Davis (2011).

free parameter, which we marginalise over to find the dipole bulk flow. We find a dipole of magnitude $U_r = 380^{+99}_{-132} \text{ km s}^{-1}$ in the direction $U_l = 295^{+18}_{-18}$ and $U_b = 14 \pm 18$ degrees. The direction of the dipole is shown in Figure 13. This is slightly slower and with a larger uncertainty than the dipole moment found by Feldman, Watkins & Hudson (2010) of $U_r = 416 \pm 78 \text{ km s}^{-1}$ in the direction $U_l = 282 \pm 11$ and $U_b = 6 \pm 6$ degrees, and is related to the larger uncertainty we find in band 1 with the catalogue method than the moments method. A comparison of measurements of the dipole is shown in Table 2.

Results from many different surveys and analysis methods appear to agree on the *direction* of the velocity dipole, at around $l = 280$ and $b = 10$ degrees, within an uncertainty radius of about 15 degrees. However, there is less consensus as to the magnitude of the dipole. The magnitude of the dipole (and the corresponding uncertainty) can depend on the depth of the survey, the treatment of outliers, and the weighting of galaxies. Even so, we can very conservatively state that the magnitude of the velocity dipole out to $100 h^{-1}\text{Mpc}$ is a factor of several times higher than the ΛCDM expectation.

5 DISCUSSION & CONCLUSIONS

In terms of understanding the high dipole moment, the main difference between the two methods we have considered here is that the catalogue method finds an excess of power in band 1 with an uncertainty which includes the ΛCDM model at the 1σ level, while the moments method finds an excess of power with an uncertainty which excludes the ΛCDM model at over the 1σ level. This is the issue we now consider. The power spectrum at these scales is closely linked to the magnitude of the dipole moment, where we similarly find a larger uncertainty with the catalogue method than the minimum variance moments result. The key to the different results are the minimum variance weights, which are designed to be sensitive to the largest scales, at the expense of small scale information. Indeed, of the sub-catalogues we analyse

	U_r [km s $^{-1}$]	U_l [degrees]	U_b [degrees]
Watkins, Feldman & Hudson (2009)	407 \pm 81	287 \pm 9	8 \pm 6
Feldman, Watkins & Hudson (2010)	416 \pm 78	282 \pm 11	6 \pm 6
Ma, Gordon & Feldman (2010)	340 \pm 130	285.1 $^{+23.9}_{-19.5}$	9.1 $^{+18.5}_{-17.8}$
Nusser & Davis (2011) (SFI++, 40 h^{-1} Mpc)	333 \pm 38	276 \pm 3	14 \pm 3
(SFI++, 100 h^{-1} Mpc)	257 \pm 44	279 \pm 6	10 \pm 6
This work	380 $^{+99}_{-132}$	295 \pm 18	14 \pm 18

Table 2. Comparison of dipole measurements within 100 h^{-1} Mpc. This work, Watkins, Feldman & Hudson (2009), Feldman, Watkins & Hudson (2010) and Ma, Gordon & Feldman (2010) all study the COMPOSITE catalogue, whereas Nusser & Davis (2011) study the SFI++ catalogue, which comprises the majority of COMPOSITE. The direction of the flow from different works agree well, although there is considerable variation in the magnitude of the flow. The magnitude of the flow can depend strongly on the depth of the survey, how galaxies at different depths are weighted, and the sensitivity of the method the fiducial power spectrum.

with the catalogue method, band 1 is best constrained by the DEEP and SMAC samples, which are the deepest of the sub-catalogues considered here. While both DEEP and SMAC are included within COMPOSITE, we find that the additional, shallower galaxies are effectively acting as noise as far as constraints on band 1 are concerned. Essentially, the minimum variance weights achieve this effect to a maximal extent: preferentially weighting the deeper galaxies with the cleanest measurement of the velocity moments, at the expense of small scale information.

On smaller scales, we also find a difference between the two methods in band 2. We find that the catalogue method agrees extremely well with the Λ CDM model, while the moments method underestimates the power. This is due to the low shear of the velocity field, which provides most sensitivity at the scales of band 2. When we analyse the full velocity catalogue, the small scale motions not modelled by the moments appear to combine to provide a constraint which again agrees extremely well with Λ CDM. In much the same way as the one band parametrisation in Macaulay et al. (2011) illustrated the difference of including only the dipole, or additionally the shear and octupole, the result in band 2 highlights the effect of considering only moments of the velocity field, or the full information available to us.

In conclusion, we find that inferring the underlying power spectrum from peculiar velocity catalogues continues the general trend of Macaulay et al. (2011): that including more detail in the velocity field improves the agreement with the Λ CDM model. Specifically, we observe good agreement with Λ CDM on scales of $k > 0.01 \text{ } h\text{Mpc}^{-1}$, although the agreement with Λ CDM in band 1 from the catalogue method is only due to the larger uncertainty than the moments method. While the high dipole moment alone may appear anomalous, when we consider the full peculiar velocity measurements, we find a power spectrum which agrees well with the Λ CDM model.

6 ACKNOWLEDGMENTS

PGF acknowledges support from STFC, BIPAC and the Oxford Martin School. HAF has been supported in part by an NSF grant AST-0807326 and by the National Science Foundation through TeraGrid resources provided by the NCSA. MJH has been supported by NSERC and acknowledges the hospitality of the Institut d’Astrophysique de Paris, and the

financial support of the IAP/UPMC visiting programme and the French ANR (OTARIE).

REFERENCES

- Abate A., Erdoğdu P., 2009, MNRAS, 400, 1541
- Abate A., Feldman H. A., 2011, ArXiv e-prints
- Ayaita Y., Weber M., Wetterich C., 2009, ArXiv e-prints
- Blake C. et al., 2010, MNRAS, 406, 803
- Cole S. et al., 2005, MNRAS, 362, 505
- da Costa L. N., Bernardi M., Alonso M. V., Wegner G., Willmer C. N. A., Pellegrini P. S., Maia M. A. G., Zaroubi S., 2000, ApJL, 537, L81
- Dressler A., Lynden-Bell D., Burstein D., Davies R. L., Faber S. M., Terlevich R., Wegner G., 1987, ApJ, 313, 42
- Feldman H. A., Watkins R., Hudson M. J., 2010, MNRAS, 407, 2328
- Hlozek R. et al., 2011, ArXiv e-prints
- Hudson M. J., Smith R. J., Lucey J. R., Branchini E., 2004, MNRAS, 352, 61
- Jaffe A. H., Kaiser N., 1995, ApJ, 455, 26
- Kashlinsky A., Atrio-Barandela F., Ebeling H., Edge A., Kocevski D., 2010, ApJL, 712, L81
- Khouri J., Wyman M., 2009, PRD, 80, 064023
- Kolatt T., Dekel A., 1995, ArXiv Astrophysics e-prints
- Kolatt T., Dekel A., 1997, ApJ, 479, 592
- Kolatt T., Dekel A., Ganon G., Willick J. A., 1996, ApJ, 458, 419
- Ma Y.-Z., Gordon C., Feldman H. A., 2010, ArXiv e-prints
- Macaulay E., Feldman H., Ferreira P. G., Hudson M. J., Watkins R., 2011, MNRAS, 391
- Masters K. L., Springob C. M., Haynes M. P., Giovanelli R., 2006, ApJ, 653, 861
- Mersini-Houghton L., Holman R., 2009, JCAP, 2, 6
- Nusser A., Davis M., 2011, ApJ, 736, 93
- Palle D., 2010, European Physical Journal C, 69, 581
- Peebles P. J. E., 1993, Principles of Physical Cosmology. Princeton University Press
- Potter W. J., Chongchitnan S., 2011, JCAP, 9, 5
- Reid B. A. et al., 2010, MNRAS, 404, 60
- Silberman L., Dekel A., Eldar A., Zehavi I., 2001, ApJ, 557, 102
- Smith R. E. et al., 2003, MNRAS, 341, 1311
- Springob C. M., Masters K. L., Haynes M. P., Giovanelli R., Marinoni C., 2009a, ApJL, 182, 474
- Springob C. M., Masters K. L., Haynes M. P., Giovanelli

- R., Marinoni C., 2009b, VizieR Online Data Catalog, 217, 20599
- Thomas S. A., Abdalla F. B., Lahav O., 2010, ArXiv e-prints
- Tully R. B., Fisher J. R., 1977, AAP, 54, 661
- Watkins R., Feldman H. A., Hudson M. J., 2009, MNRAS, 392, 743
- Zaroubi S., Bernardi M., da Costa L. N., Hoffman Y., Alonso M. V., Wegner G., Willmer C. N. A., Pellegrini P. S., 2001, MNRAS, 326, 375
- Zaroubi S., Zehavi I., Dekel A., Hoffman Y., Kolatt T., 1997, ApJ, 486, 21